

The MYB36 transcription factor orchestrates Casparian strip formation

Takehiro Kamiya^{a,1}, Monica Borghi^{a,2}, Peng Wang^a, John M. C. Danku^a, Lothar Kalmbach^b, Prashant S. Hosmani^{a,3}, Sadaf Naseer^b, Toru Fujiwara^c, Niko Geldner^b, and David E. Salt^{a,4}

^aInstitute of Biological and Environmental Sciences, University of Aberdeen, Aberdeen AB24 3UU, United Kingdom; ^bDepartment of Plant Molecular Biology, University of Lausanne–Sorge, 1015 Lausanne, Switzerland; and ^cGraduate School of Agricultural and Life Sciences, University of Tokyo, Tokyo 113-8657, Japan

Edited by Natasha V. Raikhel, Center for Plant Cell Biology, Riverside, CA, and approved June 5, 2015 (received for review April 20, 2015)

The endodermis in roots acts as a selectivity filter for nutrient and water transport essential for growth and development. This selectivity is enabled by the formation of lignin-based Casparian strips. Casparian strip formation is initiated by the localization of the Casparian strip domain proteins (CASPs) in the plasma membrane, at the site where the Casparian strip will form. Localized CASPs recruit Peroxidase 64 (PER64), a Respiratory Burst Oxidase Homolog F, and Enhanced Suberin 1 (ESB1), a dirigent-like protein, to assemble the lignin polymerization machinery. However, the factors that control both expression of the genes encoding this biosynthetic machinery and its localization to the Casparian strip formation site remain unknown. Here, we identify the transcription factor, MYB36, essential for Casparian strip formation. MYB36 directly and positively regulates the expression of the Casparian strip genes *CASP1*, *PER64*, and *ESB1*. Casparian strips are absent in plants lacking a functional *MYB36* and are replaced by ectopic lignin-like material in the corners of endodermal cells. The barrier function of Casparian strips in these plants is also disrupted. Significantly, ectopic expression of *MYB36* in the cortex is sufficient to reprogram these cells to start expressing *CASP1-GFP*, correctly localize the *CASP1-GFP* protein to form a Casparian strip domain, and deposit a Casparian strip-like structure in the cell wall at this location. These results demonstrate that MYB36 is controlling expression of the machinery required to locally polymerize lignin in a fine band in the cell wall for the formation of the Casparian strip.

Casparian strip | transcription factor | lignin | endodermis | cell wall

Plant roots are able to selectively take up both essential nutrients and water from the soil. This selectivity is provided by the endodermis, the innermost cell layer encircling the vascular system. However, to perform this function, it is critical that the Casparian strip that encircles endodermal cells works to block extracellular diffusion. Because of the vital importance of these structures for endodermal function, Casparian strips are one of the primary features of endodermal differentiation.

Casparian strips are made of a lignin polymer that is deposited as a fine band in the anticlinal cell wall, encircling endodermal cells to seal the cell wall space between them (1). This precisely situated lignin polymerization is mediated through the oxidation of monolignols by localized Peroxidase 64 (PER64) and a Respiratory Burst Oxidase Homolog F (2). This biosynthetic machinery is placed at the Casparian strip deposition site by association with Casparian strip domain proteins (CASPs). CASPs are specifically expressed in the endodermis and localize in the plasma membrane in a region in the middle of the anticlinal endodermal cell wall (3), guiding where the Casparian strip forms. Enhanced Suberin 1 (ESB1) also localizes to the Casparian strip domain, where it is required for the correct deposition of lignin and stabilization of CASPs (4). Expression of these Casparian strip-associated genes—the toolkit for the formation of Casparian strips—is regulated in both time and space during root development and marks the differentiation of the endodermis.

Here, we present our discovery of the transcriptional regulator MYB36 that orchestrates the developmentally and spatially coordinated expression of the genes necessary to position and build Casparian strips in the root endodermis. Strikingly, ectopic expression of *MYB36* is sufficient to reprogram cells to both express the genetic machinery required to synthesize Casparian strips and to locate and assemble this machinery, such that the strips develop in the correct cellular location, even though they are in cell types that do not normally form Casparian strips.

Results and Discussion

Through two different forward genetic screens using *Arabidopsis thaliana*, we isolated plants that have mutations in *MYB36*. First, in a screen of fast neutron mutagenized plants to identify genes involved in mineral nutrient and trace element homeostasis (i.e., the ionome), we identified mutant *11250* (5), now termed *myb36-1*. This mutant has multiple changes to its leaf ionome, including elevated concentrations of sodium, magnesium, and zinc and decreased calcium, manganese, and iron (Fig. S1A). The

Significance

Casparian strips play a critical role in sealing endodermal cells in the root to block uncontrolled extracellular uptake of nutrients and water. Building Casparian strips requires the construction of extracellular lignin structures that encircle cells within the cell wall and that are anchored to the plasma membranes of adjacent cells to form tight seals between them. The transcription factor we have discovered, and the set of genes it regulates, now provides us with the detailed “parts list” necessary to build Casparian strips. This finding has clear implications for better understanding the nature of tight cellular junctions in biology and also has practical implications of agricultural, offering the potential for improved water and nutrient use efficiencies and enhanced resistance to abiotic stresses.

Author contributions: T.K., T.F., N.G., and D.E.S. designed research; T.K., M.B., P.W., J.M.C.D., L.K., and S.N. performed research; T.K. contributed new reagents/analytic tools; T.K., M.B., J.M.C.D., L.K., P.S.H., N.G., and D.E.S. analyzed data; and T.K. and D.E.S. wrote the paper.

The authors declare no conflict of interest.

This article is a PNAS Direct Submission.

Freely available online through the PNAS open access option.

Data deposition: The microarray data reported in this paper have been deposited in the Gene Expression Omnibus (GEO) database, www.ncbi.nlm.nih.gov/geo (accession no. GSE62993).

See Commentary on page 10084.

¹Present address: Graduate School of Agricultural and Life Sciences, University of Tokyo, Tokyo 113-8657, Japan.

²Present address: Department of Plant Pathology, North Carolina State University, Raleigh, NC 27695-7251.

³Present address: Department of Biological Sciences, Dartmouth College, Hanover, NH 03755.

⁴To whom correspondence should be addressed. Email: david.salt@abdn.ac.uk.

This article contains supporting information online at www.pnas.org/lookup/suppl/doi:10.1073/pnas.1507691112/-DCSupplemental.

myb36-1 leaf ionome is also similar to the other known Casparian strip mutants, *esb1-1* and *caspl1;caspl3* (4), illustrated here by using principal component analyses to display the full multielement ionic phenotypes (Fig. 1A). To determine which tissues (root or shoot) are responsible for the observed alterations in the leaf ionome in *myb36-1*, we performed reciprocal grafting experiments. Plants were grafted at the 5-d-old seedling stage and allowed to grow for 5 wk before the leaf ionome was measured. The leaves of grafted plants with wild-type shoots and *myb36-1* roots had a similar ionome to that of both self-grafted and nongrafted *myb36-1* plants. However, leaves from grafted plants with *myb36-1* shoots and wild-type roots had ionomes that were indistinguishable from self-grafted or nongrafted wild-type plants (Fig. S1B). These results show that the leaf ionic phenotype of *myb36-1* is caused by a defective root function. Second, we performed an independent screen to identify genes involved in the formation of the Casparian strip. We screened ethyl methanesulfonate-mutagenized plants for individuals with no visible accumulation of CASP1-GFP when *CASP1-GFP* was expressed from the native *CASP1* promoter. Using this screen, we isolated the mutants *myb36-3* and *-4* (Fig. 1B). We observed that these *myb36* mutants have longer root hairs than wild-type (Fig. 1B), but exhibited no other obvious visible phenotypes.

To identify the causal gene in *myb36-1*, we performed genetic mapping using bulk segregant analysis (BSA-seq). We analyzed the leaf ionome of several hundred individual F2 plants from a cross between *myb36-1* in the Columbia-0 (Col-0) background and the Landsberg *erecta* accession. Based on the ionic phenotype of these F2 plants, the mutant locus was determined to be recessive. We generated two pools of plants, each containing 28 individuals with either wild-type or mutant phenotypes. The ionic phenotype of these 56 F2 plants was confirmed in the F3 generation. DNA from these two pools was extracted and sequenced on an Applied Biosystems SOLiD next-generation DNA sequencer. Short-read sequence data were aligned to the Col-0 reference genome sequence, and analysis of genome-wide heterozygosity identified a region of the genome enriched in Col-0 genotypes, which placed the causal mutation within a 22.4- to 23.6-Mb interval on chromosome V. Because the *myb36-1* mutant was generated by fast-neutron mutagenesis, which is known to cause deletion that can alter gene expression, we reasoned that genes with altered expression within our 1-Mb mapping interval would be good candidate for the causal gene in *myb36-1*. We therefore performed a microarray analysis (Affymetrix ATH1

array) to assess expression in roots of genes in our BSA-seq-mapping interval. *MYB36* (At5g57620), encoding a transcription factor, was the only gene in this interval with lower expression levels than wild-type and which is normally highly expressed in roots (Fig. S1C and D). We were unable to identify any mutations in *MYB36* between the start codon and the next gene downstream (At5g57625). However, we were also unable to amplify the promoter region of *MYB36* in *myb36-1* using several different sets of primers, suggesting the existence of a large rearrangement in the genome in this promoter region. To confirm *MYB36* as the causal gene in *myb36-1* we obtained a T-DNA insertional allele (GK-543B11) of *MYB36* (named *myb36-2*) (Fig. 1C). This T-DNA allele showed a similar leaf ionic phenotype to *myb36-1*, and F1 plants from a cross between *myb36-1* and *-2* had the mutant phenotype, demonstrating that these two mutants are allelic (Fig. S1E and F) and confirming *MYB36* as the causal gene. The *myb36-3* and *-4* alleles were also crossed with *myb36-1* and shown to be allelic as well, and DNA sequencing revealed mutations in *MYB36* in both these alleles (Fig. 1C).

To identify the cell type in which the MYB36 protein is accumulated, a GFP fusion construct was introduced into *myb36-1*. GFP was fused to the C terminus of the *MYB36* genomic sequence, which starts from 3,976 bp upstream of the start codon and extends to the end of the coding sequence. In these transgenic lines, GFP fluorescence was clearly visible in endodermal cells from the late elongation zones to the differentiation zone (Fig. 1D and G). Much weaker fluorescence was also observed in endodermal cells of the meristematic zone (Fig. 1E and F). The leaf ionic phenotype of *myb36-1* was partially rescued by this genomic sequence fused with GFP (Fig. S2A and B). Further, the *myb36-1* mutant also displayed decreased expression of genes known to be involved in Casparian strip development, including *CASP1*, *PER64*, and *ESB1*, along with defective Casparian strips and an enhanced leak into the stele of propidium iodide (PI) (Fig. S2C-E). The *MYB36* genomic sequence fused with *GFP* also partially rescued these phenotypes. This result suggests that the GFP signal observed in *myb36-1* transformed with the *MYB36-GFP* construct likely reflects the endogenous localization of MYB36.

Existing evidence suggests that *MYB36* expression is directly regulated by SCARECROW (SCR), as part of the differentiation program controlled by SHORT-ROOT (6–10). Considering the key role that Casparian strip development plays in marking endodermal differentiation, and the specific localization of MYB36-GFP to the endodermis (Fig. 1), it seemed plausible

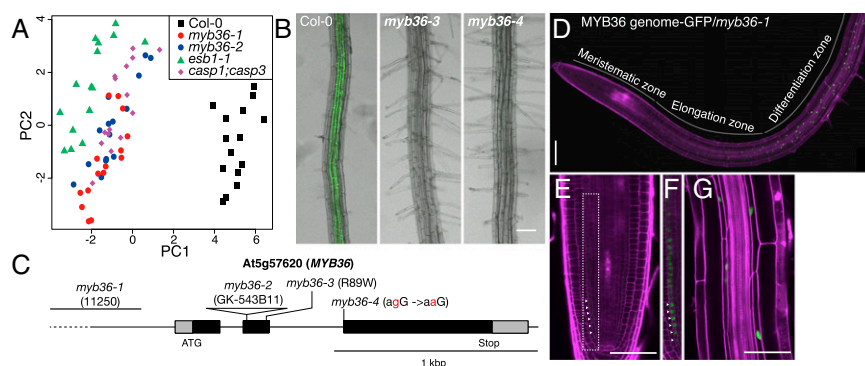


Fig. 1. Disruption of *MYB36* alters the leaf ionome and *CASP1* expression. (A) Principal component analysis based on the concentration of 20 elements in shoots ($n = 15$). (B) Mutants identified by measuring level of accumulation of *CASP1-GFP* expressed from the *CASP1* native promoter. (C) Mutation sites in the *myb36* mutants. The *myb36-1* mutant may have a large change in the promoter region because we were unable to amplify this region; *myb36-2* contains a T-DNA insertion in the second exon; *myb36-3* contains an Arg-to-Trp substitution in the second MYB domain repeat, and *myb36-4* contains a splice-site mutation after the second intron. (D–G) Endodermal localization of MYB36 using a MYB36-GFP fusion protein expressed from the *MYB36* native promoter. Magenta [propidium iodide (PI)], cell wall. E and G were taken with the same microscope settings. The dotted box in E is shown in F with the brightness of the GFP signal artificially enhanced. Arrowheads (E and F) point to examples of MYB36-GFP in the endodermal cell layer. [Scale bars: 100 μ m (B and D); 50 μ m (E and G).]

that MYB36 may be directly controlling Casparian strip formation. We used autofluorescence of the lignin within Casparian strips (1) to observe them in cleared roots of the *myb36* mutants. Autofluorescence in *myb36-1* was stronger than wild-type and more irregular in intensity than either wild-type or the known Casparian strip mutant *esb1-1* (Fig. 2A). To further identify the lignin deposition site in *myb36-1* we simultaneously visualized lignin and cell wall by treating cleared roots with PI, which stains lignin, and Calcofluor White, which stains cellulose. In *myb36*, lignin deposition was completely lacking at the endodermal cell–cell contact site, where it normally occurs to form the Casparian strip in wild-type (Fig. 2B and C). Instead, lignin-like material accumulated exclusively in the cell corners of endodermal and

cortical cells on the cortex side of the endodermis. These results indicate that MYB36 is essential for the correct localized lignin biosynthesis required to form Casparian strips. This finding contrasts with the *esb1-1* mutant in which lignin deposition still occurs at the endodermal cell–cell contact site, but the development of a continuous central lignin ring is disrupted (4) (Fig. 2B and C).

Using PI as an apoplastic tracer, we evaluated the presence of an apoplastic barrier in the *myb36* mutants. To quantify this barrier function, we counted the number of endodermal cells from the onset of elongation to the point where PI fluorescence was no longer observed in the stele-facing cell wall of the endodermis. We found that blockage of PI penetration into the stele in the *myb36* mutants was delayed compared with wild-type and was similar to the delay observed in *esb1-1* (Fig. 2D). This result indicates that the loss of the centrally located Casparian strip in *myb36* eliminates the apoplastic barrier in that region of the root. Furthermore, the ectopic lignin-like material deposited in the corners of *myb36* endodermal cells is not able to form an effective barrier to apoplastic transport. However, the diffusional barrier in *myb36* is recovered in the more mature region of the root, where suberin is normally deposited in wild-type (1).

Similar to *esb1-1* and *casp1;casp3* (4), the *myb36* mutants also showed early accumulation of suberin in the endodermis between the plasma membrane and the cell wall (Fig. 2E). Interestingly, this early accumulation of suberin was not observed in mutants made between *esb1-1* or *casp1;casp3* and *schengen3* (*sgn3*), suggesting that *SGN3*, which encodes a leucine-rich receptor like kinase, may mediate this suberin accumulation (11). By reducing transmembrane transport and enhancing apoplastic diffusion across the endodermis, the early suberin accumulation and defective Casparian strips of *myb36* could be responsible for the altered leaf ionome of this mutant (Fig. S14). Suberin deposition would be expected to reduce movement of ions across the endodermal plasma membrane, but to not affect the ions that move symplastically via plasmodesmata. Further, depending on the concentration gradient for a particular ion across the endodermis, loss of functional Casparian strips could lead to either enhanced diffusion into the stele or increased leakage back out of the stele. Such processes would be expected to give rise to the complex ionic changes observed in *myb36*.

To identify the genes regulated by MYB36, we performed a microarray analysis of genome-wide gene expression in the roots of two *myb36* alleles (*Arabidopsis* Gene 1.0 ST array). In roots from both *myb36-1* and *-2*, the expression of a common set of 39 genes was reduced, and 38 genes increased [false discovery rate (FDR) < 0.05; $|\log_2$ fold change| > 1] (Table S1). To narrow this gene set to the targets of MYB36, we limited our selection to genes normally expressed in the endodermis (12, 13) (Fig. 3A and B). Further, to eliminate those genes whose expression in *myb36* is pleiotropically affected by the loss of functional Casparian strips and ectopic suberin and lignin deposition, we eliminated genes whose expression is also altered in *esb1-1*, because *esb1-1* also lacks functional Casparian strips and develops ectopic suberin and lignin, but is not a transcriptional regulator (4) (Fig. 3A). Using quantitative PCR (qPCR), we confirmed that 30 genes, normally expressed in the endodermis, have reduced expression in *myb36* (Fig. 3C and Fig. S3). After subtracting genes showing reduced expression in *esb1-1*, a final set of 23 genes positively regulated by MYB36 was identified (Fig. 3). This set of 23 genes includes all of the *CASPs*, six *ESB-like* genes including *ESB1*, and *PER64*, representing many of the major genes identified as players in Casparian strip formation (2–4). In addition to *CASPs*, *ESBs*, and *PER64*, this gene set also contains uncharacterized protein kinase and LRR-RLK, as well as other uncharacterized proteins predicted to be localized to the extracellular space (Table S1). Together, these genes are likely to define a critical gene set required for Casparian strip formation,

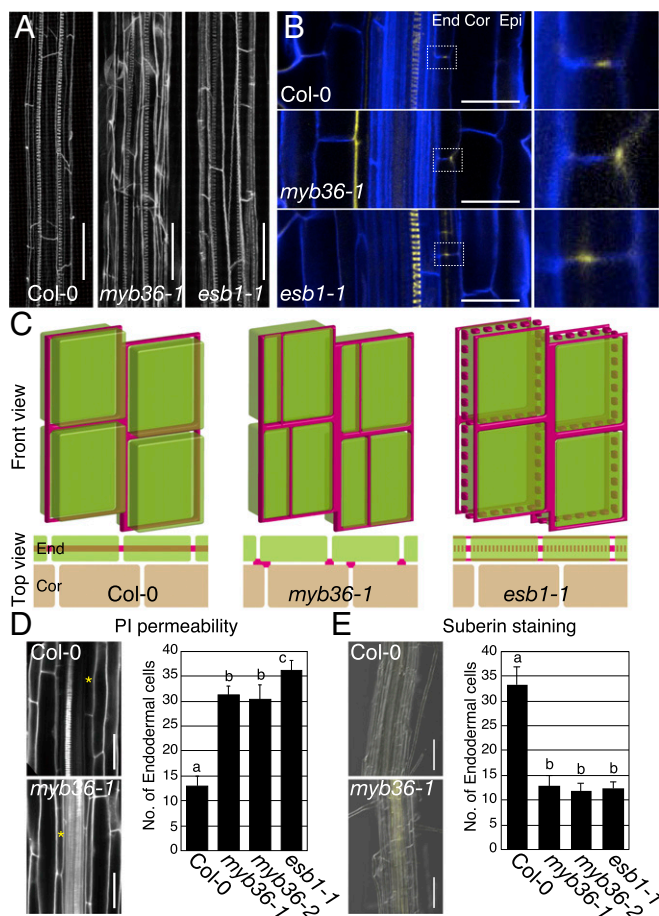


Fig. 2. Loss of Casparian strip and disruption of the apoplastic barrier in *myb36* mutants. (A) Z-stack confocal image of Casparian strip autofluorescence. Spiral structures in the center of the root are xylem. (B) Lignin (yellow) deposition site in longitudinal section. Boxed region are enlarged in *Right*. Cleared roots were stained with PI (yellow; lignin) and Calcofluor White (blue; cell wall). Although both of these dyes stain cell walls, PI primarily interacts with lignin and Calcofluor White with cellulose. Cor, cortex; End, endodermis; Epi, epidermis. (C) Schematic diagram of lignin deposition sites (magenta) in roots. Front and top views of roots are shown. (D) Casparian strip functionality was quantified by PI penetration. Asterisks in *Left* indicate the 15th endodermal cell from the onset of elongation. (E) Suberin accumulation detected with flouoral yellow 088. *Left* shows merged bright-field and flouoral yellow fluorescence (yellow; suberin) imaged around the 14th endodermal cell from the onset of elongation. The number of endodermal cells at which PI penetration into stele was blocked (D) or suberin accumulation first appeared (E) were counted from the onset of elongation. Different characters indicate significant differences by Tukey's HSD ($P < 0.05$) (D, *Right*) and Steel–Dwass test ($P < 0.05$) (E, *Right*). Data represent means \pm SD ($n = 16$ in Col-0, $n = 8$ in mutants). [Scale bars: 50 μ m (A, D, and E); 25 μ m (B).]

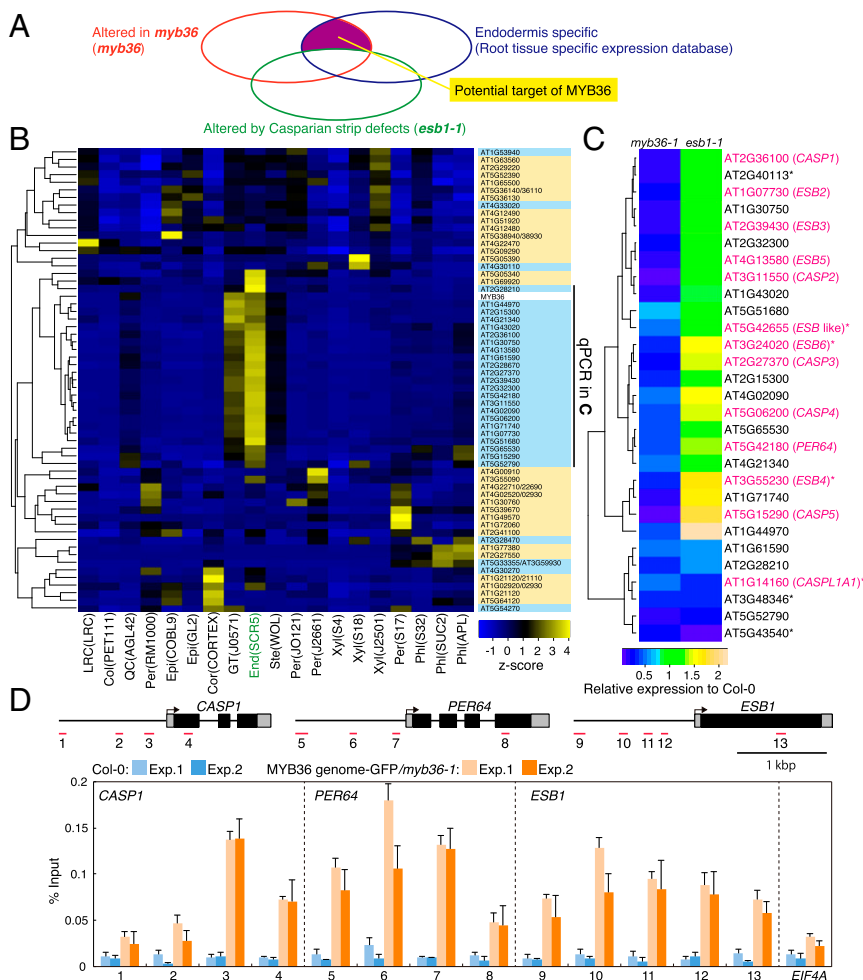


Fig. 3. MYB36 regulates Casparian strip associated genes. (A) Strategy to identify MYB36-target genes. (B) Heatmap of z-score-normalized expression of genes with $FDR < 0.05$ and $|\log_2 \text{fold change}| > 1$ in both *myb36* mutants mapped onto their radial expression pattern (12, 13). Gene IDs boxed in blue and yellow indicate genes with reduced and increased expression, respectively. End, endodermis; GT, ground tissue. Both GT and End include endodermally expressed genes. See also Table S1. (C) Heatmap showing gene expression levels in *myb36-1* and *esb1-1* relative to wild type based on qPCR results (Fig. S3). Gene IDs highlighted with an asterisk indicate genes not on the ATH1 array. Magenta shows *CASPs*, *ESBs*, and *PER64*. (D) ChIP assays using anti-GFP antibody. Red lines below the gene structure with numbers mark the location of amplicons amplified in the ChIP-qPCR. *EIF4A*, negative control. $n = 3$ from two independent experiments (Exp. 1 and 2). Bars represent mean \pm SD.

giving us important clues to the molecular mechanism of Casparian strip biogenesis.

To investigate whether MYB36 directly regulates known Casparian strip associated genes by binding to their promoters, we performed chromatin immunoprecipitation (ChIP)-qPCR against *CASP1*, *PER64*, and *ESB1* using the *MYB36 genome-GFP/myb36-1* line (Fig. 3D). MYB36 binding was found to be consistently enriched in the promoter region of these three genes relative to the wild type. Furthermore, no enrichment was observed for binding to the promoter region (1,123–1,289 bp upstream from start codon) of a ubiquitously expressed negative control gene, *EUKARYOTIC TRANSLATION INITIATION FACTOR 4A (EIF4A)*. These results indicate that MYB36 exerts its regulatory functions by associating directly with the *CASP1*, *PER64*, and *ESB1* promoters.

Casparian strip formation requires precise localization of the lignin-polymerizing machinery, which is directed by the *CASPs* in the plasma membrane (3). However, the molecular mechanisms that locate the *CASPs* to the Casparian strip formation site are unknown. To probe whether MYB36-regulated genes are involved in localization of the *CASPs*, we expressed *CASP1-mCherry* in the endodermis of *myb36-1* mutants, using the endodermally active *SCR*

promoter (3). As expected in wild type, *CASP1-mCherry* was found to be localized throughout the plasma membrane of the endodermis in the meristematic zone (Fig. S4). Further, as the root matures, *CASP1-mCherry* localization in the plasma membrane becomes restricted to a central band encircling the cell, where the Casparian strip is formed (Fig. S4 and Fig. 4A). In contrast, in the *myb36-1* mutant, *CASP1-mCherry* fluorescence does not localize into a band, but, rather, remains localized throughout the plasma membrane and also accumulates inside cells (Fig. 4A). Thus, *CASP1-mCherry* in *myb36* behaved in a similar manner to that previously observed for *CASP1-GFP* when ectopically expressed in non-endodermal cells in wild-type (Fig. 4A) (3). This result demonstrates that MYB36 in the endodermis not only regulates expression of the *CASP* genes, but also regulates expression of endodermal genes required for *CASP1* localization to the plasma membrane, a critical step in marking the site for Casparian strip deposition.

We have shown that MYB36 is necessary for the targeted deposition of lignin for the formation of Casparian strips. Next, we determined whether its expression was sufficient for Casparian strip formation. To test this hypothesis, we used transgenic lines expressing *MYB36* under the control of the β -estradiol-inducible promoter (14), with *MYB36* expression expected in all tissues.

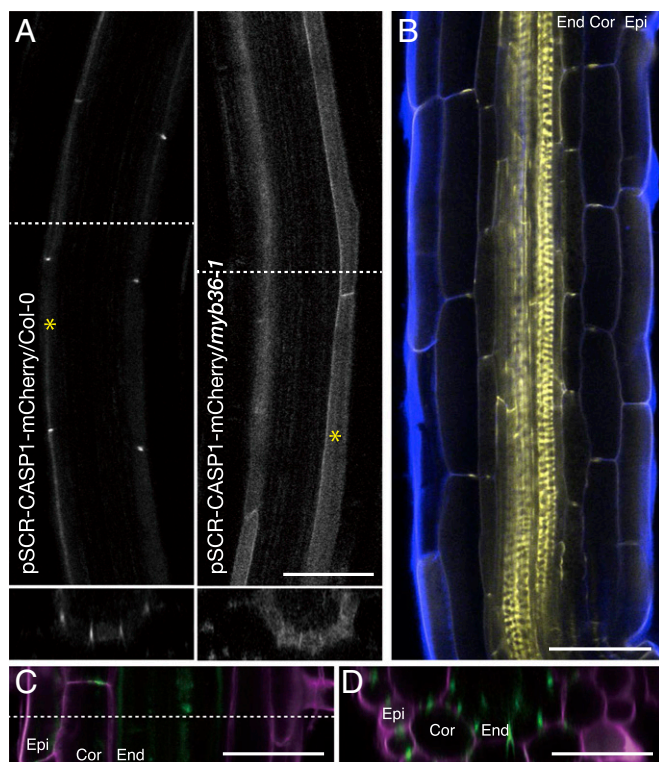


Fig. 4. MYB36 is sufficient for Casparian strip formation. (A) CASP1–mCherry localization in Col-0 and *myb36-1*. The confocal image was taken around the 20th endodermal cell (asterisks) from the onset of elongation. The images in *Lower* show radial optical sections taken from the dashed line shown in *Upper*. (B) Ectopic formation of Casparian strips in the TRANSPLANTA β -estradiol inducible line. Although both of these dyes stain cell walls, PI primarily interacts with lignin (yellow) and Calcofluor White with cellulose (blue). (C and D) CASP1–GFP (green) localization in the root of β -estradiol-treated line. Shown are longitudinal (C) and radial (D) optical sections (taken at the dashed line in C). Magenta (PI), cell wall. Cor, cortex; End, endodermis; Epi, epidermis. (Scale bars: 50 μ m.)

After β -estradiol treatment in these lines, lignin deposition was observed in the cortex, in the middle of the anticlinal cell wall in a band encircling the cells, precisely where Casparian strips would form in the endodermis (Fig. 4B and Fig. S5A and B). We confirmed that these ectopic lignin structures observed in the cortex are Casparian strip-like by demonstrating that they contain CASP1–GFP (Fig. 4C and D). Here, CASP1–GFP was expressed from the CASP1 native promoter, which is normally only active in the endodermis and is never observed in the cortex or epidermis (3). The strong and specific signal generated by CASP1–GFP also allowed us to observe Casparian strip-like patterns of CASP1–GFP accumulation in the epidermis after β -estradiol induction (Fig. 4C and D). Ectopic expression from the 35S promoter of CASP1–GFP in the cortex or epidermis has previously been shown to not be sufficient to cause the accumulation of CASP1–GFP into a Casparian strip-like domain (3). However, we show that expression of MYB36 is sufficient to drive expression of both CASP1–GFP from its native promoter and the genes required for localization of CASP1–GFP to a Casparian strip-like domain in both the cortex and the epidermis. Interestingly, the Casparian strip-like structures in the cortex have a discontinuous pattern similar to that of the *sgn3* mutant (11) (Fig. S5C). We show that SGN3 appears to not be a target for regulation by MYB36 based on our microarray data. Because SGN3 is not normally expressed in the cortex (11), this discontinuous pattern of the Casparian strip-like structure we observed when MYB36 was ectopically expressed in the cortex may be due to a lack of SGN3.

Here, we demonstrated that MYB36 regulates expression of genes critical for the localized polymerization of lignin required for the formation of Casparian strips, in both a developmentally and cell-type-specific manner. Our identification of the genes regulated by MYB36 now provides the “list of parts” needed for localizing and building Casparian strips. Further analysis of these genes should allow us to understand how these MYB36-regulated parts come together and function to overcome the engineering challenges of building Casparian strips.

Methods

Plant Materials and Growth Conditions. The Col-0 *A. thaliana* accession was used throughout the experiments. T-DNA insertion alleles of MYB36 (*myb36-2*: GK-543B11) and β -estradiol-inducible TRANSPLANTA lines (N2102512 and N2102513) (14) were obtained from the Nottingham *Arabidopsis* Stock Centre (NAS). Homozygous lines were established for GK-543B11 by using the PCR primers described in Table S2. Plants were grown on MGRM medium solidified with 1.2% (wt/vol) agar supplemented with 1% sucrose (15). After incubation for 2 d at 4 $^{\circ}$ C, plates were placed vertically, and plants were grown at 22 $^{\circ}$ C under a 16-h light/8-h dark photoperiod. For observation of Casparian strips, suberin staining by fluoral yellow 088, and PI blockage, 6-d-old seedlings were used. For β -estradiol induction, TRANSPLANTA lines were grown on MGRM medium for 5 d, and seedlings were transferred to MGRM medium containing 10 μ M β -estradiol (Sigma-Aldrich; E8875) and grown for a further 2 d.

Expression Analysis. For the microarray and qPCR analysis, root samples from 2-wk-old seedlings were used. Total RNA was prepared by using a PureLink RNA Mini Kit (Life Technologies). For the qPCR analysis, RNA was converted to cDNA by using SuperScript III (Life Technologies). The cDNA was diluted 10-fold and used for qPCR by using StepOnePlus (Life Technologies) and SYBR Select Master Mix (Life Technologies). Results of qPCR are from two independent experiments with biological duplicates. The primer sequences used are listed in Table S2. Microarray analysis was performed by NASC using the *Arabidopsis* 1.0 ST Array (Affymetrix). The microarray analysis was performed for both *myb36-1* and *-2* by using three biological replicates for each genotype. Statistical analysis of microarray data were performed by using the R bioconductor (www.bioconductor.org/). After normalization using robust multiarray average, the rank products method was performed by using the R package RankProd (16, 17). The genes satisfying the criteria (FDR < 0.05; $|\log_2$ fold change| > 1) in both of the *myb36* mutants compared with Col-0 were selected, and the cell types in which they are normally expressed were determined from the published dataset of radial expression patterns (12, 13).

Plasmid Construction and Transformation. For MYB36 localization, a MYB36 genomic DNA fragment was amplified by PCR (see Table S2 for primers), and the DNA fragment was digested and cloned into the KpnI and XhoI site of the pENTR2B dual selection vector (Life Technologies) and transferred to the destination vector pMDC107 (18) by using LR clonase (Life Technologies). For CASP1–mCherry localization in *myb36-1*, *pSCR-CASP1-mCherry* (3) was introduced into *myb36-1*. All genetic transformations were performed by using the *Agrobacterium*-mediated floral dip method. Homozygous transgenic lines were used for all experiments.

Microscope Observations. For GFP localization experiments, the FV1000 (Olympus) confocal microscope was used. Excitation and emission wavelengths were as follow: GFP, 488 and 485–545 nm; PI and mCherry, 559 and 570–670 nm. The GFP and mCherry signal was confirmed in at least five independent plants, and representative images are shown. For observation of the Casparian strip, a clearing treatment was performed as described (3, 19, 20), and cleared roots were stored in 50% (vol/vol) glycerol at 4 $^{\circ}$ C before use. Cleared roots were observed with the same settings as used for GFP. One-micrometer step-size images were taken, and z-stack images were constructed with Fiji, a distribution of ImageJ (fiji.sc/Fiji). For visualization of Casparian strips and cell wall, PI and Calcofluor White M2R (Fluorescent Brightener 28; Sigma-Aldrich; F3543) staining were performed as follows. Cleared roots (3, 19, 20) were stained with 10 μ g/mL PI in 50% (vol/vol) glycerol for 10 min and then transferred to 0.001% Calcofluor White M2R in 50% (vol/vol) glycerol. After 10 min of staining, roots were transferred to 50% (wt/vol) glycerol for observation. Confocal microscope setting for Calcofluor White M2R was excitation 405 nm, and emission was 425–475 nm. In z-stack images, 1- μ m step-size images were taken, and radial optical sections were constructed with Fiji. The autofluorescence of Casparian strip, Calcofluor White, and PI staining experiments were confirmed in at least five plants from three independent experiments, and representative images

are shown. For quantification of Casparian strips as an apoplastic barrier, the PI penetration assay was performed as described (20). The “onset of elongation” was defined as the point at which an endodermal cell in a median optical section was clearly more than twice its width (20). For suberin observation, staining by Fluoral yellow 088 was performed as described (21).

Ionic Analysis. Ionic analysis of plants grown on nutrient medium solidified with agar was performed as described (4). Briefly, plants were grown on agar-solidified medium. After 2 wk, shoots were harvested, dried at 88 °C for 20 h, and digested with concentrated nitric acid with an indium internal standard. Digested samples were diluted with 18 MΩ water and analyzed by using inductively coupled plasma (ICP)-MS (Elan DRC II; PerkinElmer) equipped with an Apex sample introduction system (Elemental Scientific). Twenty elements (Li, B, Na, Mg, P, S, K, Ca, Mn, Fe, Co, Ni, Cu, Zn, As, Se, Rb, Sr, Mo, and Cd) were monitored.

ChIP. ChIP was performed by following the protocol as described (22) with modifications as follows. Roots (100 mg fresh weight) from 11-d-old plants were cross-linked by using 4 mL of the buffer (10 mM PBS, pH 7.0, 50 mM NaCl, 0.1 M sucrose, and 1% formaldehyde) for 1 h at room temperature with the application of three cycles of vacuum infiltration (10 min under vacuum and 10 min of vacuum release). Glycine was added to a final concentration of 0.1 M to stop the cross-linking reaction, and the samples were incubated for a further 10 min. After being washed with tap water, the samples were ground to a fine powder by using a Multibeads Shocker (Yasui Kikai) at 1,500 rpm for 30 s. The powder was suspended with 2 mL of Lysis buffer [50 mM Tris-HCl, pH 7.5, 100 mM NaCl, 1% Triton X-100, 1 mM EDTA, EDTA-free Complete protease inhibitor (Roche)] and sonicated by using a Bioruptor UCD-250 (Cosmo Bio) with the following setting: mild intensity, 45 cycles (30 s ON and 30 s OFF) at 4 °C. A 100-μL sample of the chromatin sheared to between 200 and 1,500 bp was stored as the input fraction, and the rest (1.9 mL) was mixed with Dynabeads Protein G (Life Technologies)

bound with anti-GFP antibody (ab290; Abcam) and incubated for 2 h at 4 °C. The beads were washed with Lysis buffer, twice with high-salt buffer [50 mM Tris-HCl, pH 7.5, 400 mM NaCl, 1% Triton X-100, 1 mM EDTA, and EDTA-free Complete protease inhibitor (Roche)], and then with Lysis buffer. After Elution buffer (50 mM Tris-HCl, pH 8.0, 10 mM EDTA, and 1% SDS) and proteinase K (0.5 mg/mL) were added to the beads, the beads were incubated overnight at 65 °C. The DNA was purified with NucleoSpin Gel and PCR Clean-up (Macherey-Nagel) with Buffer NTB (Macherey-Nagel). Eluted solutions were used for qPCR. *E1F4A* (At3g13920) was used as a negative control, as is often used (23). The primer sequences used are listed in Table S2. Two independent experiments were performed with three biological replicates for each.

Statistical Analysis. Replicates were biological replicates from separate plants. Data in all bar graphs represent the mean ± SD. Statistical analysis was performed by using Microsoft Excel or R. No statistical methods were used to predetermine the sample size. No samples were excluded from data analysis except for ICP-MS data. For the ICP-MS data, the Suminrov–Grubb test ($P < 0.01$) was used to remove outliers as contaminations of several elements, such as Ni and Zn, which can be derived from the ICP-MS instrument. For qPCR analysis, we assumed the data came from a normally distributed population and used Tukey’s honest significant difference (HSD). For the counting experiment with PI staining and suberin accumulation (Fig. 2 *D* and *E*), Bartlett’s test was used, followed by Tukey’s HSD (Fig. 2*D*) and Steel–Dwass test (Fig. 2*E*).

ACKNOWLEDGMENTS. We thank Emiko Yokota for technical assistance; and S. Matsunaga and T. Sakamoto (Tokyo University of Science) and H. Tsukagoshi (Nagoya University) for the ChIP assay. This work was supported by National Science Foundation *Arabidopsis* 2010 Program Grant IOB 0419695; European Commission Grant PCIG9-GA-2011-291798; UK Biotechnology and Biological Sciences Research Council Grant BB/L027739/1 (to D.E.S.); Japan Society for the Promotion of Science Fellow for Research Abroad and Young Scientists (A) KAKENHI Grant-in-Aid 26712008 (to T.K.); and Japan Society for the Promotion of Science Grants 25221202 and 15H01224 (to T.F.).

- Naseer S, et al. (2012) Casparian strip diffusion barrier in *Arabidopsis* is made of a lignin polymer without suberin. *Proc Natl Acad Sci USA* 109(25):10101–10106.
- Lee Y, Rubio MC, Allassimone J, Geldner N (2013) A mechanism for localized lignin deposition in the endodermis. *Cell* 153(2):402–412.
- Roppolo D, et al. (2011) A novel protein family mediates Casparian strip formation in the endodermis. *Nature* 473(7347):380–383.
- Hosmani PS, et al. (2013) Dirigent domain-containing protein is part of the machinery required for formation of the lignin-based Casparian strip in the root. *Proc Natl Acad Sci USA* 110(35):14498–14503.
- Lahner B, et al. (2003) Genomic scale profiling of nutrient and trace elements in *Arabidopsis thaliana*. *Nat Biotechnol* 21(10):1215–1221.
- Nakajima K, Sena G, Navvy T, Benfey PN (2001) Intercellular movement of the putative transcription factor SHR in root patterning. *Nature* 413(6853):307–311.
- Sena G, Jung JW, Benfey PN (2004) A broad competence to respond to SHORT ROOT revealed by tissue-specific ectopic expression. *Development* 131(12):2817–2826.
- Levesque MP, et al. (2006) Whole-genome analysis of the SHORT-ROOT developmental pathway in *Arabidopsis*. *PLoS Biol* 4(5):e143.
- Sozzani R, et al. (2010) Spatiotemporal regulation of cell-cycle genes by SHORTRoot links patterning and growth. *Nature* 466(7302):128–132.
- Cui H, Kong D, Liu X, Hao Y (2014) SCARECROW, SCR-LIKE 23 and SHORT-ROOT control bundle sheath cell fate and function in *Arabidopsis thaliana*. *Plant J* 78(2):319–327.
- Pfister A, et al. (2014) A receptor-like kinase mutant with absent endodermal diffusion barrier displays selective nutrient homeostasis defects. *eLife* 3:e03115, 10.7554/eLife.03115.
- Birnbaum K, et al. (2003) A gene expression map of the *Arabidopsis* root. *Science* 302(5652):1956–1960.
- Brady SM, et al. (2007) A high-resolution root spatiotemporal map reveals dominant expression patterns. *Science* 318(5851):801–806.
- Coego A, et al.; TRANSPLANTA Consortium (2014) The TRANSPLANTA collection of *Arabidopsis* lines: A resource for functional analysis of transcription factors based on their conditional overexpression. *Plant J* 77(6):944–953.
- Fujiwara T, Hirai MY, Chino M, Komeda Y, Naito S (1992) Effects of sulfur nutrition on expression of the soybean seed storage protein genes in transgenic petunia. *Plant Physiol* 99(1):263–268.
- Breitling R, Armengaud P, Amtmann A, Herzyk P (2004) Rank products: A simple, yet powerful, new method to detect differentially regulated genes in replicated microarray experiments. *FEBS Lett* 573(1–3):83–92.
- Hong F, et al. (2006) RankProd: A bioconductor package for detecting differentially expressed genes in meta-analysis. *Bioinformatics* 22(22):2825–2827.
- Curtis MD, Grossniklaus U (2003) A gateway cloning vector set for high-throughput functional analysis of genes in planta. *Plant Physiol* 133(2):462–469.
- Malamy JE, Benfey PN (1997) Organization and cell differentiation in lateral roots of *Arabidopsis thaliana*. *Development* 124(1):33–44.
- Allassimone J, Naseer S, Geldner N (2010) A developmental framework for endodermal differentiation and polarity. *Proc Natl Acad Sci USA* 107(11):5214–5219.
- Lux A, Morita S, Abe J, Ito K (2005) An improved method for clearing and staining free-hand sections and whole-mount samples. *Ann Bot (Lond)* 96(6):989–996.
- Nakamichi N, et al. (2010) PSEUDO-RESPONSE REGULATORS 9, 7, and 5 are transcriptional repressors in the *Arabidopsis* circadian clock. *Plant Cell* 22(3):594–605.
- Yamaguchi N, et al. (2014) PROTOCOLS: Chromatin immunoprecipitation from *Arabidopsis* tissues. *Arabidopsis Book* 12:e0170.